Ecology Letters, (2009) **12**: 302–314 doi: 10.1111/j.1461-0248.2009.01289.x

LETTER

A link between the North Atlantic Oscillation and measles dynamics during the vaccination period in England and Wales

Mauricio Lima*
Center for Advanced Studies in Ecology and Biodiversity (CASEB), Pontificia Universidad Católica de Chile, Casilla 114-D, Santiago CP 6513677, Chile
**Correspondence: E-mail: mlima@bio.puc.cl*

Abstract

Ecologists have become aware of the role played by interannual climatic variability on the temporal dynamics of infectious diseases. In this report, I present evidence from data on measles cases in England and Wales showing that during the post-vaccination period, the interannual variability of winter weather (represented by the North Atlantic Oscillation, NAO) influences the annual dynamics of the disease. Using annual measles data from seven cities and simple logistic models, this study reveals how, after vaccination, NAO increases its effects on measles fluctuations. In addition, this study shows that vaccination may be represented as a simple vertical and lateral perturbation effect (Royama's classification), by reducing the maximum per capita growth rate and the equilibrium number of infected individuals. The results suggest that vaccination will not lead to outbreaks of measles from regular cyclic to irregular chaotic dynamics. In contrast, because of the reduction in per capita growth rates, the disease dynamics appear to be more stable than during the pre-vaccination period. The analysis of annual data on infectious diseases may be useful for detecting long-term effects of climate and complements the classical analyses and modeling based on monthly or seasonal time-step data.

Keywords

Annual data, feedback structure, logistic models, measles dynamics, North Atlantic Oscillation.

Ecology Letters (2009) 12: 302–314

INTRODUCTION

The dynamics of infectious diseases have attracted the attention of ecologists for decades (Bartlett 1957; Anderson & May 1991; Grenfell & Dobson 1995). This is because of their importance for human health and because data on childhood diseases have fuelled the development of theoretical models of population dynamics (Anderson & May 1991; Finkenstädt & Grenfell 2000). One of the most studied childhood diseases is measles because of its simple natural history and the wealth of detailed data (Grenfell & Dobson 1995). As a consequence, there is a very good understanding of the mechanisms that drive the dynamics of the infection, particularly in England and Wales, where accurate reports have been available since the Second World War (Earn *et al.* 2000; Grenfell *et al.* 2002; Bjørnstad *et al.* 2002).

Since the first studies by Bartlett (1957, 1960), there has been a firm theoretical understanding of the deterministic and stochastic factors that influence the dynamics of measles (Anderson & May 1991; Finkenstädt *et al.* 1998; Finkenstädt & Grenfell 2000; Earn *et al.* 2000; Grenfell *et al.* 2002; Bjørnstad *et al.* 2002). The classical approach is to use susceptible-infected-recovered (SIR) or susceptible-exposed-infected-recovered (SEIR) models in continuous time (Anderson & May 1991; Earn *et al.* 2000). These mechanistic models appear to capture the essential elements of measles dynamics, but because they represent continuous dynamical systems, it can be difficult to link them with available discrete time-series data. Consequently, several time series approaches have been developed in the last years for dealing with time series data of infectious diseases. For example, discrete time models using the same SEIR mechanisms have been developed to link theory on infectious disease dynamics with empirical data (Finkenstädt & Grenfell 2000; Bjørnstad *et al.* 2002). On the other hand, new statistical methods have been developed for analyzing the dynamics of infectious diseases, which are based on

stochastic differential equations and where different noise processes, such as seasonality, hidden variables and measurement error, can be included (Ionides *et al.* 2006; King *et al.* 2008).

One of the best documented dynamic patterns of measles is the transition from annual to biennial cycles in outbreaks observed in England and Wales; a transition that was caused by the decrease in birth rates following the post-World War II baby boom (Earn *et al.* 2000). Thus, one simple prediction is that countries with higher birth rates than industrialized countries will show persistent, annual dynamics (Bjørnstad *et al.* 2002; Earn *et al.* 2000). Nevertheless, complex multi-annual dynamics can be observed in countries with very high birth rates and strong seasonality in transmission rates (Ferrari *et al.* 2008). Similarly, the post-vaccination dynamics in England and Wales appears to be explained by changes in the transmission rates, which causes: (i) a switch in the periodicity and amplitude of the outbreaks (Earn *et al.* 2000); (ii) a less clear pattern of density-dependence than that observed during the pre-vaccination period (Finkenstädt *et al.* 1998); and (iii) a drop in the spatial synchrony of the epidemics (Bolker & Grenfell 1993). The general idea is that changes in birth and vaccination rates can lead measles dynamics to a regime of multiple coexisting attractors, where noise plays an important role in moving the system between the different attractors (Earn *et al.* 2000; Bauch & Earn 2003). Alternately, a recent study hypothesizes that noise amplification can explain the dynamic transitions in measles from biennial cycles to irregular fluctuations after the vaccination period (Alonso *et al.* 2007). In contrast to previous views (Earn *et al.* 2000; Bauch & Earn 2003), the irregular dynamics observed after vaccination would be caused by the amplification of the noise with transmission rates (Alonso *et al.* 2007). In support of this, a time-series model analysis of measles dynamics in Canada between pre- and post-vaccination periods shows the same model structure and dynamics in both periods (Trottier *et al.* 2006).

As in many ecological systems, infectious disease dynamics are determined to some degree by climatic variability (Rodó *et al.* 2002). In fact, recent studies on cholera (Rodó *et al.* 2002; Koelle *et al.* 2005), meningitis (Sultan *et al.* 2005), and malaria (Zhou *et al.* 2004; Pascual *et al.* 2008a,b) have detected an important role of climate in determining infectious disease dynamics. In this study, the dynamics of measles in England and Wales during the pre and post-vaccination era are analysed. I had two objectives: (i) to demonstrate that annual measles oscillations can be described by simple first order dynamics during the pre- and post-vaccination periods; and (ii) to test whether a climatic signature represented by the North Atlantic Oscillation (NAO) index and winter weather influences measles dynamics during the post-vaccination period.

MATERIAL AND METHODS

Population model

The classical approach for modeling infectious disease dynamics is the SIR or SEIR model (Anderson & May 1981). In the case of measles, the ecological population process of the disease in large populations can be represented as predator–prey dynamics between infected and susceptible individuals (Anderson & May 1981; Bjørnstad *et al.* 2002). Similar to the original Lotka–Volterra predator–prey models, the transmission rate (parameter) is directly proportional to the product of susceptible and infected individuals (βSI), which resembles the mass action principle (Berryman 1999). The cyclic nature of predator–prey oscillations observed in measles dynamics are the results of an interplay between the recruitment of new susceptible individuals (birth rate of host population) and the transmission rate, which describes how fast newly infected individuals are recruited (Earn *et al.* 2000). For a given transmission rate, high birth rates will lead to rapid replenishment of the susceptible class, and the annual dynamics of the infected class can be represented by a simple equilibrium point (Finkenstädt & Grenfell 2000; Earn *et al.* 2000; Grenfell *et al.* 2002). Lower birth rates and/or higher transmission rates lead the measles fluctuations toward a 2-year cycle (first-order oscillations) or even to multi-annual cycles typical of predator–prey dynamics (Finkenstädt & Grenfell 2000; Earn *et al.* 2000). In England and Wales, measles dynamics are characterized by annual or bi-annual cycles; therefore, I modeled the annual dynamics of infected individuals as a simple logistic process (Ricker 1954; Royama 1992):

$$I_t = I_{t-1} \cdot r_{\mathrm{m}} \cdot e^{\left(-c \cdot I_{t-1}^{a}\right)} \qquad (1)$$

where I_t is the annual number of infected individuals, r_{m} is a positive constant that represents the maximum finite reproductive rate, c is a constant that represents the competition intensity and resource depletion (susceptible individuals), and a indicates the effect of interference (how difficult it is for new individuals to become infected as the number of infected individuals increases). Alternately, the parameter r_{m} can be considered as the basic reproductive number, R_0, which is defined as the mean number of infections caused by an infected individual in a susceptible population, in an annual time scale. As a consequence, r_{m} is directly related to the susceptible numbers and the transmission rate, while parameter c is inversely related to susceptible numbers (resource dynamics). A simple prediction is that when susceptible numbers vary between years because of low birth rates and/or high transmission rates, and the resource at time $t-1$ is so depleted that it cannot recover by time $t + d$ ($d = 0, 1, 2, 3,..$), then the infected

individuals in $t-$d will influence the availability of susceptible individuals at time t. In such cases, we expect a second-order model for describing the dynamics of infected individuals (Royama 1992; Berryman 1999; Turchin 2003; Ginzburg & Colyvan 2004). In contrast, when susceptible numbers do not vary between years because of a high ratio of births to number of transmissions, annual dynamics are predicted, where it is difficult to observe large between-year variability in the infected numbers. By defining the above equation in terms of the reproduction curve (Royama 1992) or R-function (Berryman 1999), by using $R_t = \log_e (I_t/I_{t-1})$, log-transforming eqn (3), and defining the infected numbers as logarithm $X_t = log_e (I_t)$, we obtain:

$$R_t = R_m - e^{(a \cdot X_{t-1} + C)}, \quad (2)$$

where R_t is the realized per capita growth rate $R_t = \log(I_t/I_{t-1})$, $R_m = \log(r_m)$, a is the same parameter as in eqn (1), $C = \log(c)$, and $X = \log(I)$. In this model, the three parameters R_m, a and C have an explicit biological interpretation, thus we can include climatic perturbations in each parameter using the framework of Royama (1992). For example, simple additive climatic perturbations can be represented as 'vertical' effects, which shift the relative position of the R-function by changing R_m on the y-axis (Royama 1992). This can be expressed as:

$$R_t = R_m - e^{(a \cdot X_{t-1} + C)} + d \cdot \text{weather}_t . \quad (3)$$

Measles data

The measles data consisted of weekly case reports from seven cities of England and Wales during the period 1948–1987. These data are freely available at the Brian Bolker's website (electronic appendix) (Fig. 1). Annual measles notifications in England and Wales during the period 1940–2007 are also available at the *Health Protection Agency* of *UK* website (Fig. 1).

Climate data

The NAO-index used here is based on the difference in normalized sea level pressures between Ponta Delgada, Azores, Portugal and Stykkisholmur, Iceland from 1864 to 2005 for the winter period December–March (Hurrell 1995). For each of the seven localities in the UK, we obtained the monthly minimum average temperatures during winter (December–March), using the nearest meteorological station from the Met Office web site.

Statistical analyses

I fitted eqs 1–3 using the *nls* library in the program *R* by means of non-linear regression analysis (Bates & Watts 1988). In addition, I included NAO and winter minimum temperatures as a simple additive effects (eqn 3). All the models were fitted by minimizing the $AIC_c = -2 \times \log(\text{likelihood}) + 2p + 2p(p+1)/(n-p-1)$, where p is the number of model parameters and n is the sample size. Models with the lowest AIC_c values were selected. Data during the post-vaccination period were de-trended when a negative trend was detected (London and Birmingham). The models showed no convergence, therefore I used an ecological criterion for fixing the R_m parameter (maximum per capita growth rates). In many empirical time series there are few or no data at low densities. As a consequence, it is difficult to obtain information on the maximum per capita growth rates at low abundances. One way to deal with this problem is using some biological criterion to fix the parameter *a priori*, a procedure suggested by Royama (1992) and applied to different situations (Berryman & Lima 2006; Lima *et al.* 2008a,b; Estay *et al.* 2008). The lowest observed number of infected individuals was 38 in the city of Bristol and the maximum R_m value observed there was 5.2. We used this value as an approximate estimation of R_m and fixed this value at 5.5 for all models during the pre-vaccination period. Alternately, during the post-vaccination period, higher R_m values were observed in the cities of Bristol and Sheffield, which fluctuated between 2.46 and 2.86, thus I fixed this parameter at 3.0 for all cities during the post-vaccination period.

Simulated dynamics

In order to test the ability of the discrete population model to infer the underlying continuous dynamics of measles in different dynamical regimes, I simulated a SEIR model in continuous time and seasonal transmission parameter (Altizer *et al.* 2006):

$$\begin{aligned}
\frac{dS}{dt} &= \lambda \cdot (N - S) + \mu \cdot I - \beta(t) \cdot S \cdot \frac{I}{N} \\
\frac{dE}{dt} &= \beta(t) \cdot S \cdot \frac{I}{N} - \lambda \cdot E - \sigma \cdot E \\
\frac{dI}{dt} &= \sigma \cdot E - (\gamma + \mu + \lambda) \cdot I \\
R &= N - (S + E + I) \\
\beta(t) &= \beta_0 \cdot (1 + \beta_1 \cdot (\cos(2 \cdot \pi \cdot t)))
\end{aligned} \quad (4)$$

where n = population size, S = susceptible numbers, E = exposed, I = infected, R = recovered individuals, λ = birth rate, $\beta(t)$ = seasonal transmission rate, β_0 = average transmission rate, β_1 = seasonal amplitude, γ = recovery rate, and μ = mortality rate. Some degree of stochastic variability was included in the seasonal amplitude of the transmission rate using the following formulation: $\beta_1 \cdot (\cos(2 \cdot \pi \cdot t)) \cdot \varepsilon$, where ϵ is a uniformly distributed random variable that takes values between 0.002 and 2.1.

The simulations were started using the parameter values from (Altizer *et al.* 2006), which produce the classical

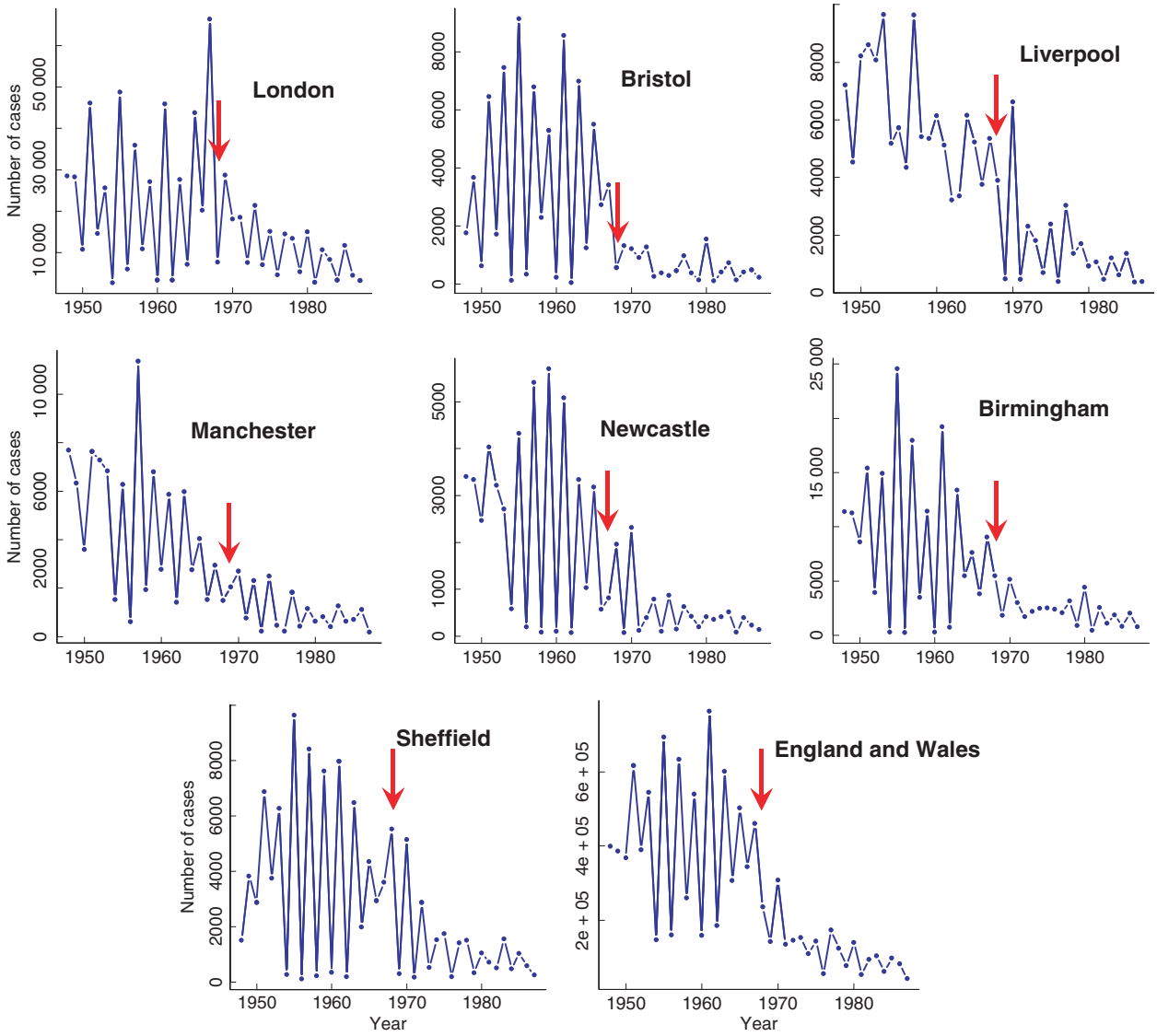

Figure 1 Time-series dynamics of measles in seven major cities of England and Wales. Annual numbers of reported cases for the period 1948–1988. The red arrow shows the year when the vaccination program started.

biennial dynamics of measles (see Table 2). The differential model was solved numerically using a fourth-order Runge–Kutta method implemented in Mathcad 8 User's Guide (1999) The basic initial parameters were $n = 5 \times 10^6$; $\lambda = 0.017$, $\beta_0 = 1250$, $\beta_1 = 0.1$, $\gamma = 73$, $\mu = 0$, $\sigma = 45.625$, and the dynamical transitions toward annual and multi-annual cycles were simulated by changing transmission rate and birth rate (see Table 2). The annual simulated dynamics from model 4 was analysed using classic tools from time series diagnosis. The first step in the analysis was to use diagnostic tools for determining the order or dimension of the time series. Subsequently, a linear autoregressive model for each simulation was fitted as:

$$R_t = \ln\left(\frac{N_t}{N_{t-1}}\right) = A + B_1 \cdot X_{t-1} + B_2 \cdot X_{t-2} + \varepsilon_t \qquad (5)$$

where $X = \log_e(N)$, n = population density, $R_t = \log_e(N_t/N_{t-1})$ is the realized logarithmic per capita rate of change over a year, and ϵ_t is a random stochastic variable $(0, \sigma^2)$. Parameters of the linear model were estimated in the program R using the *stats* library. The estimated Partial Rate Correlation Function (PRCF): (i) is the partial correlation between R and X_{t-d}, $d = 1, 2 \ldots 3$, providing an estimate of the order of the autoregressive process (Berryman 1999; Berryman & Turchin 2001). PRCF (i) can be interpreted as a measure of the importance – or relative contribution – of feedback at lag d to the determination of R. After the

diagnosis, the logistic model from eqn (3) and the delayed-time (second-order) logistic model (Royama 1992; Table 2) were used for fitting the annual simulated dynamics of the continuous time SEIR model.

RESULTS

Infected dynamics were adequately represented by a simple non-linear logistic first-order process during the pre-vaccination period (1948–1967) (Table 1). The logistic model explained 93% of the variance of infected dynamics in Sheffield, while in Liverpool explained only 35% (Table 1). However, in most of the cities, a simple Ricker model explained 93–64%, and using the pooled data for England and Wales, the endogenous factors explained 92% of the measles dynamics (Table 1). During the post-vaccination period (1968–1988), the pure logistic model explained between 55% (Bristol) and 77% (Newcastle), and for England and Wales together, the endogenous factors explained only 77% of the measles dynamics (Table 1). Thus, the endogenous component of the dynamics was reduced in almost all cities during the post-vaccination period.

In contrast, the proportion of variance explained by the winter weather (NAO or winter minimum temperatures) in the measles dynamics increased during the post-vaccination period (Tables 1 and 2). For example, the residuals of the pure endogenous models showed a significant negative correlation with NAO in Bristol, Liverpool, Newcastle and Sheffield (Table 2), with the minimum average temperature during December in London, Bristol, Manchester, Sheffield and Birmingham (Table 2). In addition, residual variation showed significant negative effects of January minimum temperatures in London and Birmingham, and negative effects of March minimum temperatures in Newcastle (Table 2). On average, model residuals were negatively correlated with NAO and December minimum average temperatures (Table 2).

During the pre-vaccination period, including NAO in the logistic models improved the explained variance up to 2% only (Table 1), while during the post-vaccination period NAO and winter weather terms improved the explained variance from 3 to 21%, depending on the city (Table 1). In the England and Wales pooled data, including the NAO term improved the explained variance of the model by 8% (Table 1). The AIC_c values and Akaike weights provide strong support for the role of NAO as an important exogenous perturbation in Bristol, Liverpool, Newcastle and Sheffield (Table 1). A similar result is observed with the December–January minimum temperatures in London and Birmingham (Table 1), but in Manchester the models with NAO or December minimum temperature were similar to that without weather effects (Table 1). Similarly, the model for England and Wales together including NAO effects is almost nine times more likely than the model without the climate effect (Table 1). The overall effect of vaccination on measles *R*-function appears to be a decrease in the equilibrium point and the maximum per capita growth rate R_m (Fig. 2).

Observed annual measles dynamics before and after vaccination can be characterized as a classical first-order feedback structure (Fig. 3a,b), which supports the choice of the Ricker's model with one time lag. The simulated dynamics using the SEIR model shows that the same dynamic process is observed in the parameter region of biennial and annual cycles (Fig. 3c,d). However, when the SEIR model is simulated using lower birth and/or transmission rates (vaccination) the PRCF shows a clear increase in the order of the dynamics, indicating that second-order annual models are better for describing this dynamic process (Fig. 3e–h; Table 3). The SEIR model simulations represented as annual dynamics show that biannual and annual cycles ($\beta = 1250$; $\lambda = 0.017$; $\lambda = 0.035$ and $\lambda = 0.06$; Table 3) can be expressed as simple first-order logistic models (Fig. 4). When transmission rates and birth rates are low, as expected during the vaccination period ($\beta = 625$; $\beta = 500$; $\lambda = 0.01$; $\lambda = 0.006$; $\lambda = 0.004$; Table 3), the annual output of the SEIR continuous model is best represented by second-order logistic annual models (Table 3; Fig. 5).

DISCUSSION

The results of this study give a new perspective on measles dynamics, a perspective where the annual variability is described by a simple logistic model of population dynamics. First of all, the analysis suggests that vaccination does not lead measles dynamics to a regime of multiple coexisting attractors. In contrast, the ecological system during the post-vaccination period appears to be the same as during the pre-vaccination period: first-order feedback dynamics characterized by a single and stable lower equilibrium number of infected individuals, and a reduced maximum per capita growth rate. Previous studies using the classical SEIR modeling approach predict complex multi-annual outbreak dynamics, caused by an interplay between seasonality, noise, and the magnitude of transmission and birth rates (Olsen *et al.* 1988; Earn *et al.* 2000; Bauch & Earn 2003). However, Alonso *et al.* (2007) hypothesized that high noise amplification can explain the dynamic transitions in measles dynamics from biennial cycles to irregular fluctuations after the vaccination period. The results of this study are consistent with the proposition of Alonso *et al.* (2007). A recent study by Ferrari *et al.* (2008) supports the idea that complex multi-annual dynamics can be generated by an interaction of high birth rates and seasonality in transmis-

Table 1 Population dynamics models fitted to time-series of measles in seven cities of England and Wales

Models for measles dynamics	Parameters												
	b	*a*	*C*	*d*	*e*	r^2	AIC_c	ΔAIC_c	w_i	w_i/w_j	Log (likelihood)	*k*	Shapiro–Wilk normality test
London (1948–1967)													
+ NAO	5.50	0.33	−1.54			0.83	51.67	0.00	0.82	1.00	−22.09	3	$W = 0.95$, $P = 0.39$
	5.50	0.32	−1.49	−0.04		0.83	54.66	2.99	0.18	4.45	−21.99	4	$W = 0.95$, $P = 0.31$
London (1968–1988)													
+NAO	3.00	0.55	−3.96			0.80	28.59	7.65	0.18	47.33	−10.44	3	$W = 0.95$, $P = 0.42$
	3.00	0.57	−4.16	−0.08		0.82	29.34	8.40	0.13	66.58	−9.13	4	$W = 0.97$, $P = 0.78$
+ Temperature December	3.00	0.65	−5.05	−0.13		0.86	25.83	4.89	0.72	11.53	−7.37	4	$W = 0.98$, $P = 0.96$
+ Temperature January	3.00	0.67	−5.21	−0.14		0.86	24.27	3.33	1.58	5.28	−6.59	4	$W = 0.95$, $P = 0.37$
+ Temperature December and January	**3.00**	**0.77**	−6.25	−0.11	−0.13	**0.91**	**20.94**	**0.00**	**8.33**	**1.00**	−2.97	**5**	$W = 0.94$, $P = 0.32$
Bristol (1948–1967)													
+ NAO	5.50	0.43	−1.71			0.89	62.09	2.32	0.24	3.20	−26.71	3	$W = 0.97$, $P = 0.65$
	5.50	0.42	−1.60	−0.26		0.92	59.77	0.00	0.70	1.00	−23.89	4	$W = 0.96$, $P = 0.52$
Bristol (1968–1988)													
+NAO	3.00	0.36	−1.16			0.56	51.14	7.71	0.02	47.12	−21.72	3	$W = 0.95$, $P = 0.41$
	3.00	**0.50**	**−2.01**	**−0.32**		**0.76**	**43.44**	**0.00**	0.96	1.00	**−16.18**	**4**	$W = 0.96$, $P = 0.60$
+ Temperature December	3.00	0.45	−1.79	−0.17		0.63	51.49	8.05	0.017	55.98	−20.20	4	$W = 0.97$, $P = 0.82$
+ Temperature December and March	3.00	0.55	−2.65	−0.16	−0.19	0.67	53.41	9.97	0.006	146.43	−19.20	5	$W = 0.97$, $P = 0.84$
Liverpool (1948–1967)													
+ NAO	5.50	0.13	0.55			0.36	17.54	0.000	0.83	1.00	−5.02	3	$W = 0.96$, $P = 0.64$
	5.50	0.14	0.54	0.003		0.36	20.70	3.16	0.17	4.82	−5.02	4	$W = 0.97$, $P = 0.69$
Liverpool (1968–1988)													
+NAO	3.00	0.33	−1.03			0.69	48.23	2.67	0.20	3.79	−20.25	3	$W = 0.96$, $P = 0.67$
	3.00	**0.45**	**−2.12**	**−0.22**		**0.77**	**45.57**	**0.00**	**0.76**	**1.00**	**−17.25**	**4**	$W = 0.96$, $P = 0.61$
+ Temperature December	3.00	0.45	−2.18	−0.11		0.69	51.27	5.70	0.043	17.28	−20.09	4	$W = 0.97$, $P = 0.78$
+ Temperature December and March	3.00	0.53	−2.98	−0.12	−0.17	0.71	54.07	8.50	0.010	70.21	−19.53	5	$W = 0.96$, $P = 0.56$
Manchester (1948–1967)													
+ NAO	5.50	0.26	−0.49			0.69	50.22	0.00	0.76	1.00	−21.36	3	$W = 0.96$, $P = 0.50$
	5.50	0.28	−0.65	0.09		0.70	52.50	2.28	0.24	3.12	−20.92	4	$W = 0.95$, $P = 0.40$
Manchester (1968–1988)													
+NAO	3.00	0.43	−1.88			0.63	50.94	0.04	0.50	1.012	−21.62	3	$W = 0.98$, $P = 0.94$
	3.00	**0.50**	**−2.29**	**−0.19**		**0.70**	**50.91**	**0.00**	**0.51**	**1.00**	**−19.92**	**4**	$W = 0.97$, $P = 0.87$
+ Temperature December	3.00	0.52	−2.60	−0.19		0.69	51.27	0.36	0.42	1.20	−20.10	4	$W = 0.97$, $P = 0.86$
+ Temperature December and March	3.00	0.65	−3.69	−0.18	−0.21	0.74	53.16	2.21	0.17	3.01	−19.00	5	$W = 0.96$, $P = 0.64$

Table 1 *(Continued)*

Models for measles dynamics	Parameters												
	b	*a*	*C*	*d*	*e*	r^2	AIC_c	ΔAIC_c	w_i	w_i/w_j	Log (likelihood)	*k*	Shapiro–Wilk normality test
Newcastle (1948–1967)													
+ NAO	5.50	0.41	−1.36			0.86	62.96	0.00	0.80	1.00	−27.73	3	$W = 0.96$, $P = 0.62$
	5.50	0.42	−1.50	0.087		0.86	65.67	2.71	0.21	3.88	−27.50	4	$W = 0.98$, $P = 0.93$
Newcastle (1968-1988)													
+NAO	3.00	0.45	−1.56			0.77	49.01	5.77	0.05	17.81	−20.66	3	$W = 0.97$, $P = 0.86$
	3.00	**0.46**	**−1.67**	**−0.25**		**0.86**	**43.25**	**0.00**	**0.94**	**1.00**	**−16.09**	**4**	$W = 0.95$, $P = 0.50$
+ Temperature December	3.00	0.46	−1.69	−0.08		0.77	52.87	9.62	0.008	122.73	−20.40	4	$W = 0.98$, $P = 0.96$
+ Temperature December and March	3.00	0.55	−2.37	−0.08	−0.29	0.81	53.07	9.82	0.007	135.85	−19.04	5	$W = 0.99$, $P = 0.99$
Birmingham (1948–1967)													
+ NAO	5.50	0.43	−2.12			0.88	61.36	0.00	0.70	1.00	−26.93	3	$W = 0.91$, $P = 0.07$
	5.50	0.45	−2.33	0.14		0.88	63.08	1.72	0.30	2.35	−26.20	4	$W = 0.88$, $P = 0.02$
Birmingham (1968–1988)													
+NAO	3.00	0.63	−3.71			0.91	14.34	1.527	0.26	2.14	−3.32	3	$W = 0.95$, $P = 0.46$
	3.00	0.62	−3.68	−0.06		0.92	14.92	2.10	0.19	2.86	−1.92	4	$W = 0.94$, $P = 0.33$
+ Temperature December	**3.00**	**0.65**	**−3.92**	**−0.07**		**0.94**	**12.82**	**0.00**	**0.55**	**1.00**	**−0.87**	**4**	$W = 0.98$, $P = 0.93$
+ Temperature January	3.00	0.65	−3.91	−0.06		0.93	14.43	1.61	0.25	2.24	−1.68	4	$W = 0.96$, $P = 0.66$
+ Temperature December and January	3.00	0.66	−4.00	−0.05	−0.03	0.94	15.53	2.71	0.14	3.88	−0.27	5	$W = 0.98$, $P = 0.98$
Sheffield (1948–1967)													
+ NAO	5.50	0.47	−2.08			0.92	50.49	0.00	0.822	1.00	−21.50	3	$W = 0.94$, $P = 0.27$
	5.50	0.47	−2.06	−0.03		0.92	53.56	3.07	0.18	4.65	−21.44	4	$W = 0.94$, $P = 0.24$
Sheffield (1968–1988)													
+ NAO	3.00	0.49	−2.25			0.77	49.73	1.70	0.30	2.33	−21.01	3	$W = 0.99$, $P = 0.99$
	3.00	**0.50**	**−2.39**	**−0.20**		**0.83**	**48.04**	**0.00**	**0.70**	**1.00**	**−18.48**	**4**	$W = 0.96$, $P = 0.66$
+ Temperature December	3.00	0.54	−2.75	−0.17		0.81	50.75	2.71	0.16	3.88	−19.68	4	$W = 0.97$, $P = 0.75$
+ Temperature December and March	3.00	0.59	−3.24	−0.17	−0.11	0.82	53.85	5.81	0.032	18.29	−19.43	5	$W = 0.98$, $P = 0.89$
England and Wales (1948–1967)													
+NAO	4.59	0.43	−3.99			0.92	15.73	0.00	0.85	1.00	−2.53	4	$W = 0.96$, $P = 0.46$
	4.46	0.44	−4.17	−0.011		0.92	19.26	3.53	0.15	5.83	−2.48	5	$W = 0.95$, $P = 0.45$
England and Wales (1968–1988)													
+NAO	3.00	0.53	−5.06			0.76	15.12	4.38	0.10	8.94	−3.71	3	$W = 0.96$, $P = 0.55$
	3.00	**0.55**	**−5.33**	**−0.09**		**0.84**	**10.75**	**0.00**	**0.90**	**1.00**	**0.17**	**4**	$W = 0.93$, $P = 0.15$

a, non-linearity coefficient; *b*, maximum finite reproductive rate; *C*, equilibrium point; *d*, coefficients for climatic effects; r^2, coefficient of determination; AIC_c, Akaike's information criterion corrected for small sample bias; ΔAIC_c, differences in AIC_c; w_i, Akaike weights; w_i/w_j, evidence ratios; *k*, number of estimated parameters; *W*, the value of the Shapiro–Wilk statistic test of normality in model residuals; *P*, the *P*-value for the test; bold face indicates best models including climatic effects.

Table 2 Pearson's product-moment correlation coefficients between the weather variables (NAO and minimum monthly temperatures in winter) and the residuals of model 2 (Logistic model without climatic covariables) fitted to the time series of each city

	NAO	Temperature December	Temperature January	Temperature February	Temperature March
London	−0.36 (P = 0.14)	−0.56 (P = 0.015)	−0.58 (P = 0.012)	0.051 (P = 0.84)	−0.023 (P = 0.93)
Bristol	−0.60 (P = 0.008)	−0.40 (P = 0.095)	−0.16 (P = 0.54)	0.087 (P = 0.73)	−0.34 (P = 0.17)
Liverpool	−0.54 (**P = 0.020**)	−0.25 (P = 0.32)	0.27 (P = 0.29)	0.20 (P = 0.42)	−0.23 (P = 0.36)
Manchester	−0.37 (P = 0.12)	−0.42 (**P = 0.081**)	0.10 (P = 0.70)	0.05 (P = 0.84)	−0.36 (P = 0.14)
Newcastle	**−0.63 (P = 0.005)**	−0.22 (P = 0.38)	−0.04 (P = 0.86)	0.18 (P = 0.48)	**−0.44 (P = 0.07)**
Birmingham	−0.38 (P = 0.12)	**−0.50 (P = 0.037)**	**−0.40 (P = 0.10)**	−0.18 (P = 0.47)	−0.13 (P = 0.60)
Sheffield	**−0.49 (P = 0.04)**	**−0.44 (P = 0.066)**	0.16 (P = 0.53)	0.40 (P = 0.10)	−0.25 (P = 0.31)
Average	−0.48	−0.40	−0.093	0.11	−0.25

NAO, North Atlantic Oscillation.
Boldfaces are P-values lower than 0.1.

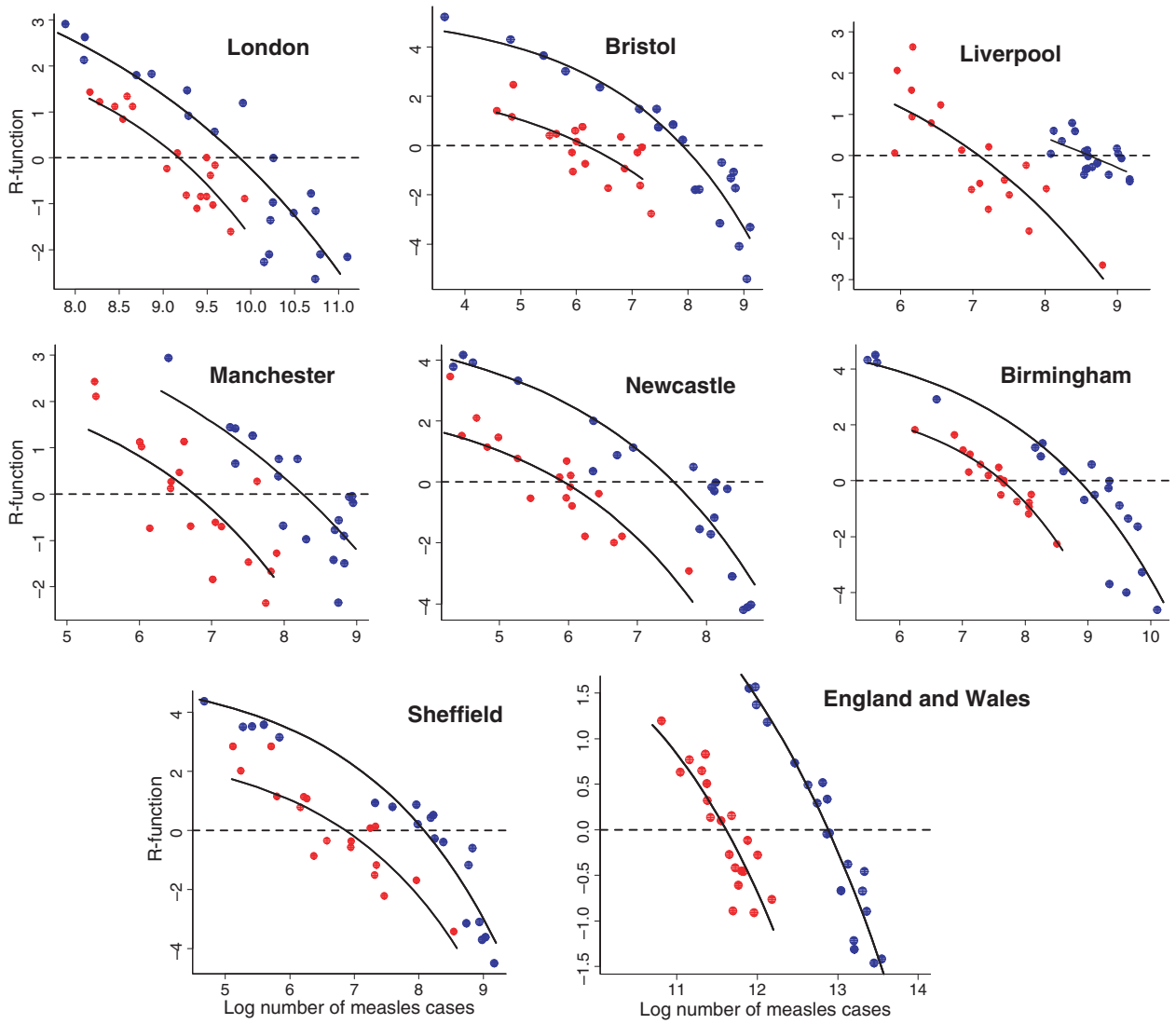

Figure 2 Lateral and vertical displacement of the R-functions due to the effects of vaccination program. R-functions [eqn (2)] fitted to data from 1948–1967 (blue) and 1968–1988 (red) for the seven cities and all of England and Wales. See Table 1 for statistics.

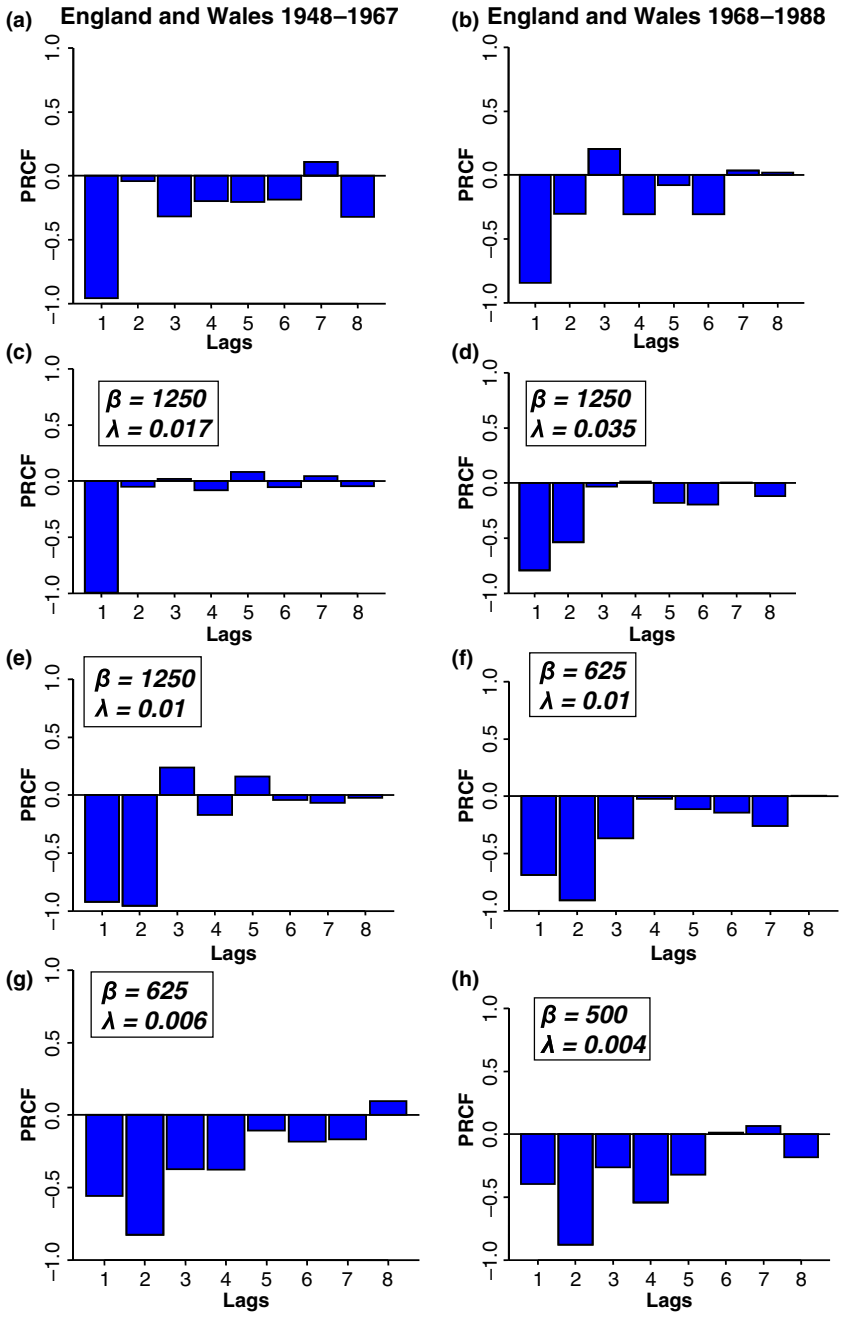

Figure 3 Partial correlation between R and X_{t-d}, with d the lag in the feedback response for observed and annual simulated measles dynamics. (a) observed time series of number of cases in England and Wales before vaccination; (b) observed time series of number of cases in England and Wales after vaccination; (c) simulated biannual cycles of measles cases using the, susceptible-exposed-infected-recovery (SEIR) model (eqn 4) and $\beta = 1250$, $\lambda = 0.017$; (d) simulated annual cycles of measles cases using the SEIR model (eqn 4) and $\beta = 1250$, $\lambda = 0.035$; (e) simulated 3-year cycles of measles cases using the SEIR model (eqn 4) and $\beta = 1250$, $\lambda = 0.01$; (f) simulated multi-annual cycles of measles cases using the SEIR model (eqn 4) and $\beta = 625$, $\lambda = 0.01$; (g) simulated multi-annual cycles of measles cases using the SEIR model (eqn 4) and $\beta = 625$, $\lambda = 0.006$; (h) simulated multi-annual cycles of measles cases using the SEIR model (eqn 4) and $\beta = 500$, $\lambda = 0.004$.

sion rates. However, if the infected–susceptible dynamics are perceived as a predator–prey system, multi-annual cycles (with a period > 2 years) can only be generated when the predator (infected individuals) has a high per capita growth rate relative to its prey (susceptible individuals) and/or higher attack rates (Berryman 1999). In the SEIR modeling perspective, this is equivalent to diseases with high transmission rates and low recovery rates relative to the birth rates (or recruitment rates) of susceptible individuals (Keeling & Rohani 2008). In sum, when susceptible individuals are removed due to infection at a faster rate than they are recruited by birth, multi-annual predator-prey-like cyclic dynamics are expected.

This study indicates that vaccination can be perceived as a vertical and lateral perturbation effect on the R-function of measles dynamics (Royama 1992) (Fig. 2). A vertical perturbation effect because vaccination reduces the maximum per capita growth rates of infected individuals and this quantity is proportional to the number of susceptible individuals, and the transmission and recovery rates. Also, a

Table 3 Logistic and lagged logistic population dynamics models fitted to the simulated annual time-series of measles using the continuous time SEIR model

Models for simulated measles dynamics	Parameters						
	R_m	a	a_1	C	r^2	AIC_c	ΔAIC_c
$R_t = R_m - e^{(a \cdot X_{t-1} + C)}$							
1. $\beta = 1250$; $\lambda = 0.017$	2.28	0.92		−9.29	0.992	—	—
2. $\beta = 1250$; $\lambda = 0.035$	2.44	0.73		−7.53	0.874	—	—
3. $\beta = 1250$; $\lambda = 0.060$	0.42	3.00		−37.16	0.633	—	—
4. $\beta = 1250$; $\lambda = 0.010$	1.14	1.56		−16.21	0.856	136.92	83.30
5. $\beta = 625$; $\lambda = 0.010$	0.69	1.37		−14.56	0.465	−57.53	211.84
6. $\beta = 625$; $\lambda = 0.006$	0.78	0.79		−8.04	0.310	−24.55	161.99
7. $\beta = 500$; $\lambda = 0.004$	0.52	0.63		−6.56	0.166	37.63	265.15
$R_t = R_m - e^{(a \cdot X_{t-1} + a_1 \cdot X_{t-2} + C)}$							
4a. $\beta = 1250$; $\lambda = 0.010$	2.62	0.72	0.35	−9.94	0.939	53.62	0.00
5a. $\beta = 625$; $\lambda = 0.010$	1.28	0.69	0.74	−14.50	0.925	−269.37	0.00
6a. $\beta = 625$; $\lambda = 0.006$	2.62	0.11	0.34	−3.43	0.860	−186.54	0.00
7a. $\beta = 500$; $\lambda = 0.004$	12.02	−0.028	0.080	2.00	0.943	−227.52	0.00

SEIR, susceptible-exposed-infected-recovery.
(Equation 4) and different combinations of transmission rates (β) and birth rates (λ). a, non-linearity coefficient; a_1, 1-year lagged coefficient; b, maximum finite reproductive rate; C, equilibrium point; r^2, coefficient of determination; AIC_c, Akaike's information criterion corrected for small sample bias; ΔAIC_c, differences in AIC_c. Models were run for 1000 annual time steps and the first 900 years were discarded.

lateral perturbation effect because vaccination reduces the total number of susceptible individuals available to be infected, and this is can be thought of as a reduction in the carrying capacity of the system. Because the dynamics of infected and susceptible individuals are the result of an interplay between transmission (β), recovery (γ), and recruitment (λ) rates, we need to understand how these rates are affected in order to predict the effect of vaccination. From an ecological point of view, if the influence of vaccination affects proportionally these parameters, one would expect similar dynamics before and after vaccination (in terms of the order of the feedback structure), with changes only in the equilibrium number of infected individuals and the maximum per capita growth rates. Observing the change in measles dynamics in England and Wales during the pre- and post-vaccination periods, it is clear that fluctuations in the number of infected individuals became stabilized after vaccination (Fig. 1), which is predicted by the logistic theory when R_m is reduced (Berryman 1999). In fact, time-series analyses of infectious diseases before and after vaccination suggest the existence of a similar underlying endogenous structure (Trottier *et al.* 2006). Indeed, the observed reduction in R_m was $\sim$ 45% (from 5.5 to 3.0) and the reduction in the equilibrium number or infected individuals was $\sim$ 70% (from 369,535 to 111,302 individuals), which is proportional to the average vaccination coverage during the period 1968–1985 (54%) (http://www.hpa.org.uk/web/HPAweb&HPAwebStandard/HPAweb_C/1195733786957). It is important to notice that vaccination has changed the dynamics of another disease in a dramatic manner, such as in the whooping cough case, where multiannual 4–5 year cycles were triggered after vaccination (Rohani *et al.* 2002). As far I know, no mechanistic explanation has been proposed for this change in the dynamic structure during the vaccination era.

An interesting finding of this study is that climate – represented by NAO and winter minimum temperatures – has noticeable influence on the measles dynamics during the post-vaccination period. The irregular dynamics observed during that period appears to be influenced by winter weather, represented by NAO or minimum average temperature during December. Alonso *et al.* (2007) proposed that the irregular dynamics observed after vaccination could be caused because the noise amplification of the system changes with the transmission rates. It is important to notice that irregular noisy dynamics are also observed before the vaccination in Liverpool due to the high recruitment rates observed in that city. Therefore, it seems that the ratio between how fast infected individuals produce new infections and the recruitment of susceptible individuals is what determines the degree of noise influence. When the endogenous dynamics becomes more stable, the role of noise appears to be more important (see Fig. 4a–c). This is consistent with the observed increase in the importance of winter weather after vaccination. Alternately, NAO itself has experienced low-frequency variability: the NAO index was more negative during the period 1965–1985 than other decades (Hurrell 1995). Negative NAO values are associated with cooler and drier winters in northern Europe (Hurrell 1995), which may influence the transmission rate by

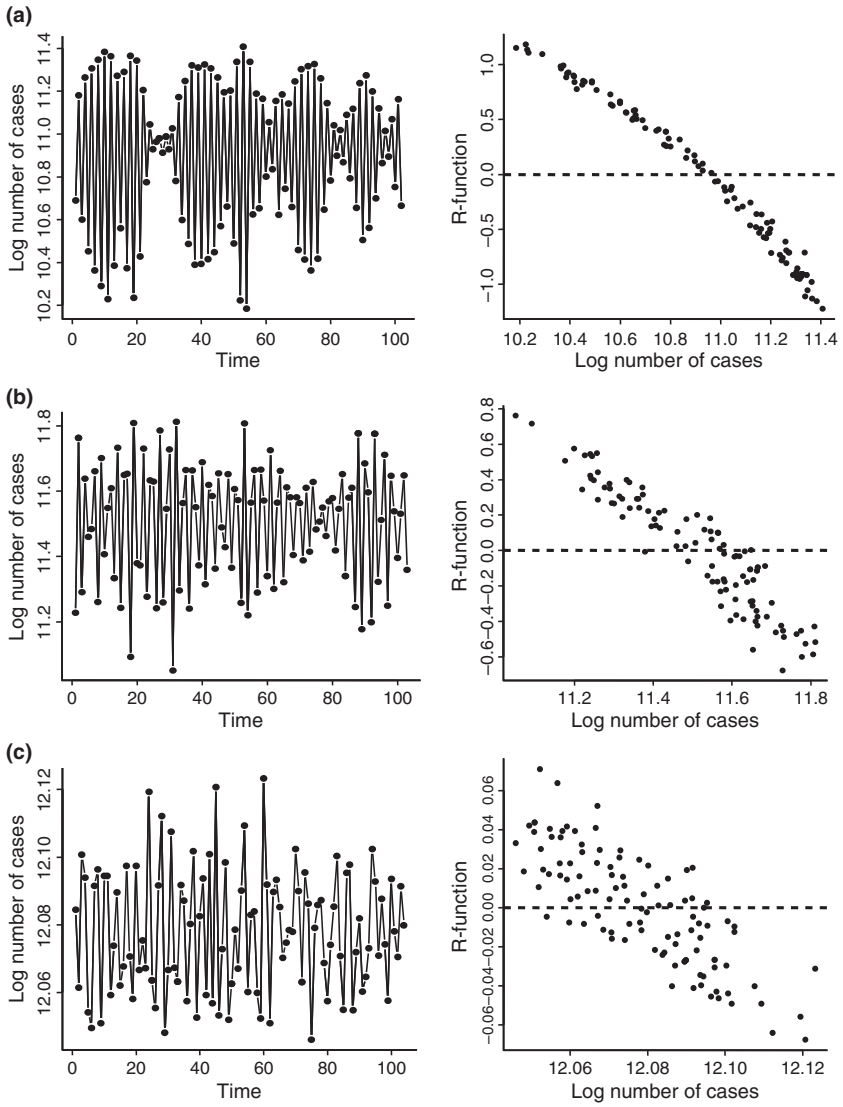

Figure 4 (Left side) Time series plot of the simulated log numbers of infected individuals using the susceptible-exposed-infected-recovery model (eqn 4) and (right side) plot of the per capita growth rate of infected individuals against the log number of infected cases. (a) biannual cycles (β = 1250; λ = 0.017); (b) annual cycles (β = 1250; λ = 0.035); (c) annual cycles (β = 1250; λ = 0.06).

lowering the immune defense in children, or changing their social behavior.

The seasonal variability of transmission rate in the UK is complex and seems to be determined by other factors beyond the pure effect of the school period (Finkenstädt & Grenfell 2000; Bjørnstad *et al.* 2002). For example, transmission rates tend to be high after the start of the school period, then decline toward the end of the year, and show their peak during late December and early January. After this major peak, transmission rates decline again until the eastern holidays and show a minor peak during April–May before declining to very low values during the summer vacation period (Finkenstädt & Grenfell 2000; Bjørnstad *et al.* 2002). It is interesting to note that the minimum average temperature during December appears to be the most important variable compared with temperatures recorded during other winter months. It is likely that the highest peak in transmission rate observed during late December-early January in the UK is influenced by the minimum temperatures of December. Under this hypothesis, winter weather may influence the transmission rate in this period and may cause inter-annual variability in measles dynamics. Also, note that minimum average temperature during March shows a weak but consistent negative correlation with model residuals (Table 2), suggesting that weather during late winter-early spring may be related with the other peak in transmission rates observed from bi-weeks 9 to 11 (Finkenstädt & Grenfell 2000).

In the same vein, long-term changes in transmission rates associated with climate change have been reported for malaria and cholera (Koelle & Pascual 2004; Pascual *et al.* 2008a,b). Some recent studies have related El Niño Southern Oscillation (ENSO) events with changes in cholera prevalence (Rodó *et al.* 2002; Koelle *et al.* 2005),

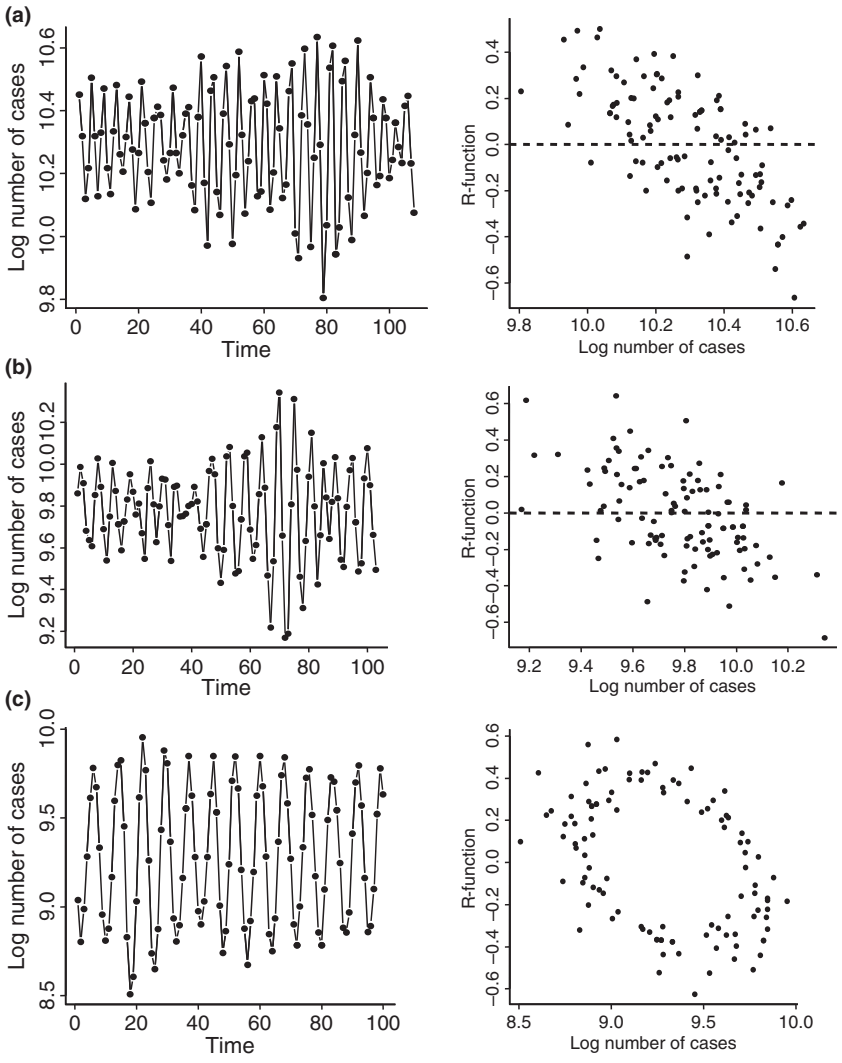

Figure 5 (Left side) Time series plot of the simulated log numbers of infected individuals using the susceptible-exposed-infected-recovery model (eqn 4) and (right side) plot of the per capita growth rate of infected individuals against the log number of infected cases. (a) multi-annual cycles (β = 625; λ = 0.01); (b) multi-annual cycles (β = 625; λ = 0.006); (c) multi-annual cycles (β = 500; λ = 0.004).

rainfall variability with malaria in east Africa (Zhou *et al.* 2004; Pascual *et al.* 2008a,b), and climate variability with outbreaks of meningitis in west Africa (Sultan *et al.* 2005). Although most of these studies are based on statistical relationships between disease prevalence and climate variation, some are based on the use of an explicit epidemiological model, which suggests that climatic trends may influence disease transmission rate (Koelle & Pascual 2004; Pascual *et al.* 2008a,b). The climate effects detected in this report suggest that, after vaccination, winter weather is an important exogenous factor that influences measles dynamics, likely through its effects on the seasonal pattern of transmission rates.

In this study, I propose the use of a simple logistic model based on annual measles dynamics, instead of the classical SEIR models based on weekly or monthly time-step data. My analysis provides an alternative view of the consequences of vaccination on measles dynamics in England and Wales, and highlights the role of climate after the vaccination period. Most of the infectious diseases are strongly influenced by seasonality (Altizer *et al.* 2006), but the same argument is valid for many ecological systems, such as insects and small rodents. In many populations in which seasonality is important, simple models based on annual time-step data have been developed and used for understanding and prediction (Royama 1992; Berryman 1999). This study shows that ecological models based on the annual dynamics of an infectious disease can be used as an alternative for analyzing and understanding disease dynamics. My analysis resolves previous contradictory findings about measles dynamics.

ACKNOWLEDGEMENTS

This study was funded by FONDAP grant 1501–0001 (Program 2). I am particularly indebted to M. Pascual and two anonymous referees for their comments on this report and to F. Jaksic.

REFERENCES

Alonso, A., McKane, A.J. & Pascual, M. (2007). Stochastic amplification in epidemics. *J. R. Soc. Interface.*, 4, 575–582.

Altizer, S., Dobson, A., Hosseini, P., Hudson, P., Pascual, M. & Rohani, P. (2006). Seasonality and the dynamics of infectious diseases. *Ecol. Lett.*, 9, 467–484.

Anderson, R. & May, R. (1981). The population dynamics of microparasites and their invertebrate hosts. *Phil. Trans. R. Soc. Lond. B Biol. Sci.*, 291, 451–524.

Anderson, R. & May, R. (1991). *Infectious Diseases of Humans: Dynamics and Control*. Oxford University Press, USA.

Bartlett, M. (1957). Measles periodicity and community size. *J. R. Stat. Soc.*, 120, 48–70.

Bartlett, M. (1960). The critical community size for measles in the United States. *J. R. Stat. Soc.*, 123, 37–44.

Bates, D. & Watts, D. (1988). *Nonlinear Regression Analysis and its Applications*. Wiley, New York.

Bauch, Chr.T. & Earn, D.J.D. (2003). Transients and attractors in epidemics. *Proc. R. Soc. Lond. B Biol. Sci.*, 270, 1573–1578.

Berryman, A.A. (1999). *Principles of Population Dynamics and Their Application*. Stanley Thornes Ltd., Cheltenham, UK.

Berryman, A.A. & Turchin, P. (2001). Identifying the density-dependent structure underlying ecological time series. *Oikos*, 92, 265–270.

Berryman, A.A. & Lima, M. (2006). Deciphering the effects of climate on animal populations: diagnostic analysis provides new interpretation of Soay sheep dynamics. *Am. Nat.*, 168, 784–795.

Bjørnstad, O., Finkenstädt, B. & Grenfell, B. (2002). Dynamics of measles epidemics: estimating scaling of transmission rates using a time series sir model. *Ecol. Monogr.*, 72, 169–184.

Bolker, B. & Grenfell, B. (1993). Chaos and biological complexity in measles dynamics. *Proc. Biol. Sci.*, 251, 75–81.

Earn, D., Rohani, P., Bolker, B. & Grenfell, B. (2000). A simple model for complex dynamical transitions in epidemics. *Science*, 287, 667–670.

Estay, S., Lima, M. & Harrington, R. (2009). Climate mediated exogenous forcing and synchrony in populations of the oak aphid in the UK. *Oikos*, 118, 175–182.

Ferrari, M.J., Grais, R.F., Bharti, N., Conlan, A.J.K., Bjornstad, O.N., Wolfson, L.J. *et al.* (2008). The dynamics of measles in sub-Saharan Africa. *Nature*, 451, 679–684.

Finkenstädt, B. & Grenfell, B. (2000). Time series modelling of childhood diseases: a dynamical systems approach. *J. R. Stat. Soc., Ser C. Appl Stat.*, 49, 187–205.

Finkenstädt, B., Keeling, M. & Grenfell, B. (1998). Patterns of density-dependence in measles dynamics. *Proc. R. Soc. Lond. B Biol Sci.*, 265, 753–762.

Ginzburg, L. & Colyvan, M. (2004). *Ecological Orbits: How Planets Move and Populations Grow*. Oxford University Press, New York, USA.

Grenfell, B. & Dobson, A. (1995). *Ecology of Infectious Diseases in Natural Populations*. Cambridge University Press, Cambridge, New Jersey.

Grenfell, B., Bjørnstad, O. & Finkenstädt, B. (2002). Dynamics of measles epidemics: scaling noise, determinism, and predictability with the tsir model. *Ecol. Monogr.*, 72, 185–202.

Hurrell, J.W. (1995). Decadal trends in the North Atlantic Oscillation: regional temperatures and precipitation. *Science*, 169, 676–679.

Ionides, E.L., Bretó, C. & King, A.A. (2006). Inference for nonlinear dynamical systems. *Proc. Natl Acad. Sci. USA*, 103, 18438–18443.

Keeling, M.J. & Rohani, P. (2008). *Modeling Infectious Diseases in Humans and Animals*. Princeton University Press, Princeton, New Jersey.

King, A.A., Ionices, E.L., Pascual, M. & Bouma, M.J. (2008). Inapparent infections and cholera dynamics. *Nature*, 454, 877–881.

Koelle, K. & Pascual, M. (2004). Disentangling extrinsic from intrinsic factors in disease dynamics: a nonlinear time series approach with an application to cholera. *Am. Nat.*, 163, 901–913.

Koelle, K., Rodó, X., Pascual, M., Yunnus, Md. & Mostafa, G. (2005). Refractory periods and climate forcing in cholera dynamics. *Nature*, 436, 696–700.

Lima, M., Harrington, R., Saldaña, S. & Estay, S. (2008a). Nonlinear feedback processes and a latitudinal gradient in the climatic effects determine green spruce aphid outbreaks at the UK. *Oikos*, 117, 951–959.

Lima, M., Morgan Ernest, S.K., Brown, J.H., Belgrano, A. & Stenseth, N.C. (2008b). Chihuahuan desert kangaroo rats: nonlinear effects of population dynamics, competition, and rainfall. *Ecology*, 89, 2594–2603.

Mathcad 8 User's Guide (1999). *MathSoft, Inc*. Cambridge, Mass, USA.

Olsen, L.F., Truty, G.L. & Schaffer, W.M. (1998). Oscillations and chaos in epidemics: a non-linear dynamic study of six childhood diseases in Copenhagen, Denmark. *Theo. Pop. Bio.*, 33, 344–370.

Pascual, M., Cazelles, B., Bouma, M.J., Chaves, L.F. & Koelle, K. (2008a). Shifting patterns: malaria dynamics and rainfall variability in an African highland. *Proc. R. Soc. Lond. B Biol Sci.*, 275, 123–132.

Pascual, M., Chaves, L.F., Rodo, X., Cash, B. & Yunus, Md. (2008b). Predictability of endemic cholera: the role of climate variability and disease dynamics. *Climate Res.*, 36, 131–140.

Ricker, W. (1954). Stock and recruitment. *J. Fisheries Res. Board Can.*, 11, 559–623.

Rodó, X., Pascual, M., Fuchs, G. & Faruque, A.S.G. (2002). ENSO and cholera: a nonstationary link related to climate change? *Proc. Natl Acad. Sci. USA*, 20, 12901–12906.

Rohani, P., Keeling, M.J. & Grenfell, B.T. (2002). The interplay between determinism and stochasticity in childhood disease. *Am. Nat.*, 159, 469–481.

Royama, T. (1992). *Analytical Population Dynamics*. Chapman & Hall, London, UK.

Sultan, B., Labadi, K., Guegan, J. & Janicot, S. (2005). Climate drives the meningitis epidemics onset in West Africa. *PLoS Med*, 2, e6, 0043–0049.

Trottier, H., Phillipe, P. & Roy, R. (2006). Stochastic modeling of empirical time series of childhood infectious diseases data before and after mass vaccination. *Emer. T. Epid.*, 3, doi:10.1186/1742-7622-3-9.

Turchin, P. (2003). *Complex Population Dynamics: A Theoretical/empirical Synthesis*. Princeton University Press, Princeton, USA.

Zhou, G., Minakawa, N., Githeko, A.K. & Yan, G. (2004). Association between climate variability and malaria epidemics in the East African highlands. *Proc. Natl. Acad. Sci. USA*, 101, 2375–2380.

Editor, Bernd Blasius
Manuscript received 20 November 2008
First decision made 31 December 2008
Second decision made 24 January 2009
Manuscript accepted 28 January 2009